Determination of the Thermal Lens of a PPKTP Crystal Based on Thermally Induced Mode-Mismatching

Yajun Wang, Zhixiu Li, Yaohui Zheng, and Jing Su

***Abstract*— We present a method for determining the thermal focal length of periodically poled potassium titanyl phosphate (PPKTP) through measuring the variation in the mode-matching efficiency between the seed beam and the TEM_{00} eigenmode of an external optical cavity. The eigenmode size of the external optical cavity changes with the thermal focal length originating from the absorption of PPKTP inside the external optical cavity, whereas the fundamental wave injected into the external optical cavity keeps the geometrical size unchanged, which continuously deteriorates the mode-matching efficiency between the fundamental wave and external optical cavity's eigenmode. Thus, we can obtain the thermal focal length at different power levels of a harmonic wave according to the corresponding mode-matching efficiency. The measurement is more sensitive to the absorbed power in the material, which can be of high precision under intense pumping. Finally, the uncertainty of the method is analyzed.**

***Index Terms*— Lasers, frequency doubled, thermal lensing, thermal effects, optical resonators.**

I. Introduction

DUE to its prominently high nonlinear coefficient, high damage threshold and good flexibility, the periodically poled potassium titanyl phosphate (PPKTP) crystal is an attractive nonlinear material for versatile devices, e.g., second harmonic generation (SHG) [1]–[4] and optical parametric oscillation (OPO) [5]–[7]. The former is a universal method for frequency transformation from the near infrared to visible spectral range, and the latter is the most effective technique for squeezed-state generation and frequency downconversion. These two processes are nonlinear interactions and are accompanied by absorptions of fundamental waves and harmonic waves [8]–[12], which make a fraction of the two waves deposit energy as heat and cause a temperature gradient along the radial direction of the PPKTP crystal. The inhomogeneous temperature distribution induces a temperature-dependent variation of the refractive index (dn/dT), stress dependence of the refractive index and thermal expansion [12]–[15], which cause thermal lensing [3], [16], thermal birefringence [17], [18] and thermally induced phase mismatching (TIPM) in the crystal [17], [19], [20]. Due to the small Youngs modulus and thermal expansion of KTP compared with dn/dT, the contribution of stress-induced changes can be ignored [17], and the thermal effect is only considered as the contribution of dn/dT. The remaining two harmful effects will reduce the beam quality, make the resonator unstable (thermal lens), perturb the phase-matching condition, and reduce the phase-matching temperature acceptance bandwidth and efficiency of the nonlinear interaction (TIPM) [12], [17]. In particular, as the wavelength of the harmonic wave decreases, the absorption coefficient of the PPKTP crystal becomes high [21], which will result in more serious thermal effects to further reduce the output quality of the optical cavity and must be thoroughly considered and characterized for cavity design to achieve optimum efficiency of the SHG and OPO processes [22]–[24].

M. Sabaeian et al. theoretically researched the TIPM and thermal lens effects in detail using Maxwells coupled wave equations for the SHG of Gaussian beams [17], [19], [20], and they demonstrated that the two effects are important for representing the characteristics of the thermal effect and optimizing an optical system. In this work, we experimentally focus on the thermal focal length measurement of HW in a PPKTP crystal. The thermal focal length in a gain medium has already been studied in detail using a variety of techniques to obtain efficient lasing operation [25], [26]. Koechner et al. measured the thermal lens effect using a probe beam technique [27], [28]. A probe beam is a collinear beam that is passed through the crystal with a pump laser, and then the thermal focal length is determined by measuring the beam waist distance from the exit end face of the crystal. The thermal lens effect can also be obtained by measuring the far-field and near-field waists of the output beam of a laser using a CCD [29]. Song et al. reported a method for measuring the thermal lens effect based on an unstable cavity technique [30]. The unstable cavity is composed of two plane mirrors, and at the point of extinguishing the laser, the cavity length equals the thermal focal length. It also is determined by measuring the output of the oscillation beam waist size from a laser using the rate equation method [31]. Bows et al. reported a method

Manuscript received August 15, 2016; revised October 9, 2016 and November 11, 2016; accepted November 15, 2016. Date of publication December 15, 2016; date of current version January 5, 2017. This work was supported in part by the National Natural Science Foundation of China under Grant 61575114, Grant 61574087, Grant 11654002, and Grant 11504220, in part by the National Key Research and Development Program of China under Grant 2016YFA0301401, in part by the Program for Outstanding Innovative Teams of Higher Learning Institutions of Shanxi, in part by the Natural Science Foundation of Shanxi Province, China under Grant 2015021022, and in part by the Program for Sanjin Scholar of Shanxi Province. *(Corresponding author: Yaohui Zheng.)*

The authors are with the State Key Laboratory of Quantum Optics and Quantum Optics Devices, Collaborative Innovation Center of Extreme Optics, Institute of Opto-Electronics, Shanxi University, Taiyuan 030006, China (e-mail: wangyajun_166@163.com; lizhixiu1083@163.com; yhzheng@sxu.edu.cn; jingsu@sxu.edu.cn)

Color versions of one or more of the figures in this paper are available online at http://ieeexplore.ieee.org.

Digital Object Identifier 10.1109/JQE.2016.2640229

called holographic lateral shearing interferometry (HLSI) for determining the thermal focal length of an astigmatic thermal lens [32]. All of these above works focused on the thermal focal length of the gain medium, but the thermal effect of the nonlinear crystal was neglected. Although the probe beam and HLSI techniques can also be used to measure the thermal focal length of the PPKTP crystal, they cannot represent the actual operating conditions of both SHG and OPO. Recently, Bogan et al. proposed a method for measuring the thermal lens of optical components by observing the power of second-order modes [33], which is only appropriate for weak thermal lens measurements.

Considering the strong absorption of the PPKTP crystal at 397.5 nm, our group has taken note of its thermal effect during the process of frequency doubling at 795 nm and theoretically compared the thermal focal length of the linear standing-wave cavity and ring cavity for external cavity frequency doubling [3]. However, experimental measurements of the thermal focal length were not performed.

Our main contribution in this work is to quantify the thermal focal length of the PPKTP crystal based on the relationship between the mode-matching efficiency of an external optical cavity and the thermal focal length. The basis of the proposed mechanism is as follows: the eigenmode size of the external optical cavity changes with the thermal focal length originating from the absorption of light by PPKTP inside the external optical cavity, whereas the geometry of the injected fundamental wave of the external optical cavity is kept constant, which alters the mode-matching efficiency between the fundamental wave and external optical cavity's eigenmode. Thus, we can obtain the thermal focal length at different powers of harmonic waves according to the corresponding mode-matching efficiency. The uncertainty in the thermal focal length results primarily arises from the measurement accuracy of the mode-matching efficiency. The experimental setup, which includes an external optical cavity and a PPKTP crystal inside the external optical cavity, is similar to the actual cavity structure of SHG or OPO.

II. Measurement Principle

A simple external optical cavity includes two reflecting mirrors and a nonlinear crystal. Under ideal conditions, the cavity's eigenmode size is determined by the cavity length and the curvature radius of the two reflecting mirrors, and it remains constant. Nevertheless, in an actual frequency upconversion and downconversion setup, the fundamental wave and harmonic wave, which interact with each other in the nonlinear medium, are partially absorbed to heat the PPKTP crystal, forming a thermal lens inside the cavity. Compounding matters, this thin lens is sensitive to the power variation of the FW and HW, which acts as a dynamical intracavity optical lens that varies with the absorbed power to indicate the eigenmode size of the cavity and make it deviate from the initial value and vary with the change of the fundamental wave and harmonic wave power. In our thermal focal length measurement, the fundamental wave acts as a seed beam with low power and can be associated with the eigenmode of the external optical cavity. When the seed beam waist remains constant and the eigenmode of the cavity changes with the dynamic lens, the mode-matching efficiency between the two modes will be lowered by the updated eigenmode size. Therefore, we can establish the relationship between the thermal focal length and mode-matching efficiency with an intermediate variable of the eigenmode at different absorbed powers. In this paper, we will focus on the frequency conversion process between 795 nm and 397.5 nm, corresponding to the transitions at the rubidium D1 line [34]. To simplify the measurement, a weak seed beam with its polarized direction perpendicular to the optical axis of the PPKTP is injected into the cavity to avoid the interaction between the fundamental and harmonic waves, while the absorption at 795 nm is less than 150 ppm/cm [35], whose contribution to the thermal effect can be neglected. Although the multiple-pass mechanism of the FW and HW in the cavity with an intracavity crystal is possible by simultaneously coupling nonlinear, heat and phase with Maxwells and heat equations [17], to simplify the measurement process in this work, we only consider the single-pass condition of the HW. Then, the thermal focal length primarily related to dn/dT in the material can be deduced from the heat equation and total phase change accumulated by single pass laser light [3], [16],

$$f_{th} = \frac{\pi K_c \omega_0^2}{P_{2\omega}(1 - e^{-\alpha l})\frac{dn}{dT}} \tag{1}$$

where $P_{2\omega}$ is the harmonic wave power, K_c is the thermal conductivity of the material, dn/dT is the thermo-optic coefficient, ω_0 is the beam waist of the harmonic wave, α is the absorption coefficient of the harmonic wave, and l is the length of the crystal. For PPKTP, the parameters are $\alpha = 18.6\%$/cm [3], $K_c = 13$ W/m/K and dn/dT=1.6×10^{-5}/K [36]. The thermal focal length is inversely proportional to the harmonic wave power; hence, an increase in the harmonic wave power will result in a more serious thermal focal length.

When an input Gaussian beam is mode-matched to an external optical cavity, there are three reasons to excite higher-order modes (mode mismatching): input beam misalignment, waist position mismatching, and waist size mismatching [37]. The influence of the former two on the mode mismatching can be minimized by optimizing the initial mode-matching efficiency and improving the point stability and spatial mode, e.g., inserting a mode cleaner into the optical path of the seed beam. Consequently, the mode-matching efficiency value is dominated by the waist size mismatching.

If we assume that the relationship between the seed beam (a pure TEM_{00} mode, ω_{s0}) and fundamental mode of the cavity (ω_{e0}) is $\omega_{s0} = \omega_{e0}(1 + \varepsilon)$, then the electric field of the seed beam can be expanded by the cavity eigenmodes in polar coordinates [37],

$$\psi_s(r) = A[u_{eo}(r) + \varepsilon u_{e1}(r) + higher\ order\ terms] \tag{2}$$

where ε is the difference between the radius of the seed beam and fundamental mode of the cavity; the electric fields of the cavity eigenmode are $u_{eo}(r)$ and $u_{e1}(r)$ for the zero-order and first-order eigenmodes of the cavity, respectively. In this case, the mode-matching efficiency of each higher-order mode can be obtained by a power ratio of a TEM_{mn}

and the total eigenmode of the cavity [38],

$$\kappa_{mn} = \frac{P_{mn}}{\sum_{i,j} P_{ij}} \tag{3}$$

and the power can be implied by the electric field part in equation (2) [39]. It also implies that $\sum_{m,n=0}^{\infty} \kappa_{mn} = 1$.

In general, the various spatial modes of the cavity have nondegenerate resonant frequencies, and the fundamental and higher-order modes in the cavity correspond to different transmission peaks with a frequency difference of $\delta\nu = k\nu_0$ ($\nu_0 = \frac{c}{2l}\cos^{-1}[1 - \frac{l}{R}]$, c is the speed of light and R is the curvature radius of the cavity mirror, k=m+n for a certain TEM $_{mn}$ mode) [37]. Different frequencies correspond to different resonant cavity lengths; hence, we can distinguish the TEM$_{mn}$ modes by scanning the cavity length, and the intensities of the cavity's transmission peaks can be detected by a photodetector in real time. Therefore, κ_{mn} are read out from different transmission peaks of the cavity. In real experiments, we always pay attention to the mode-matching efficiency to the TEM$_{00}$ mode, and we define the total mode-matching efficiency of higher-order modes as a mode-mismatching efficiency to the fundamental one ($\varepsilon = 1 - \kappa_{00}$). The variation in the mode-matching efficiency in our resonator reflects the change of the TEM$_{00}$ eigenmode, which is directly related to the thermal focal length of the nonlinear medium.

The relationship between the thermal focal length (f_{th}) and eigenmode waist radius (ω_{e0}) of the optical cavity can be constructed using ABCD matrix theory, in which f_{th} acts as an intracavity thin lens, but its focal length changes with the harmonic wave power. The result is shown as a dashed curve in Fig. 1, from which we can find that the thermal focal length monotonically enlarges the ω_{e0}. At the same time, the relationship between the mode-matching efficiency and ω_{e0} can also be constructed under the premise that the seed beam waist radius (ω_{s0}) remains unchanged. The power ratio κ_{00} can also be equivalent to the spatial mode-matching efficiency (κ_{00}) to the cavity TEM$_{00}$ eigenmode (ω_e) in (x,y,z) coordinates as [38],

$$\kappa_{00} = \frac{|\Pi_{\alpha=x,y} \int_0^l dz \int \psi_s(\alpha, z) u_{e0}(\alpha, z) d\alpha|^2}{\Pi_\alpha \left\{\int_0^l dz \int |\psi_s(\alpha, z)|^2 d\alpha\right\} \left\{\int_0^l dz \int |u_{e0}(\alpha, z)|^2 d\alpha\right\}} \tag{4}$$

$$\psi_s(\alpha, z) = \frac{1}{\sqrt{\pi}\omega_s(z)} \exp(-\frac{\alpha^2}{\omega_s^2(z)}) \tag{5}$$

$$u_{e0}(\alpha, z) = \frac{1}{\sqrt{\pi}\omega_{e0}(z)} \exp(-\frac{\alpha^2}{\omega_{e0}^2(z)}) \tag{6}$$

In an optical cavity without astigmatism, the mode sizes are the same in the sagittal and tangential planes of the cavity, and both the seed beam and cavity eigenmode are a Gaussian beam; subsequently, the corresponding eigenmode can be expressed by

$$\omega_{s(e)}^2(z) = \omega_{s0(e0)}^2 \left\{1 + \left(\frac{(z - z_a)}{z_{s(e)}}\right)^2\right\} \tag{7}$$

where ω_s is the beam radius of the seed beam; L_c is the length of the external optical cavity; ω_s(z) and ω_e(z) are the beam radii of the seed beam and external optical cavity eigenmode at the longitudinal distance z, respectively; ω_{s0} (a constant value of 38.9 μm) and ω_{e0} are those of the waist radius; z_a is that of the beam waist position; $z_s = \pi\omega_{s0}^2/\lambda$; $z_e = \pi\omega_{e0}^2/\lambda$; and λ is the wavelength of the seed beam. Then, the TEM$_{00}$ mode-matching efficiency is simplified as,

$$\kappa_{00} = 16\{\frac{\{\int_0^{L_c} \frac{1}{\omega_s^2(z)+\omega_e^2(z)} dz\}^2}{\int_0^{L_c} \frac{1}{\omega_s^2(z)} dz \times \int_0^{L_c} \frac{1}{\omega_e^2(z)} dz}\}^2 \tag{8}$$

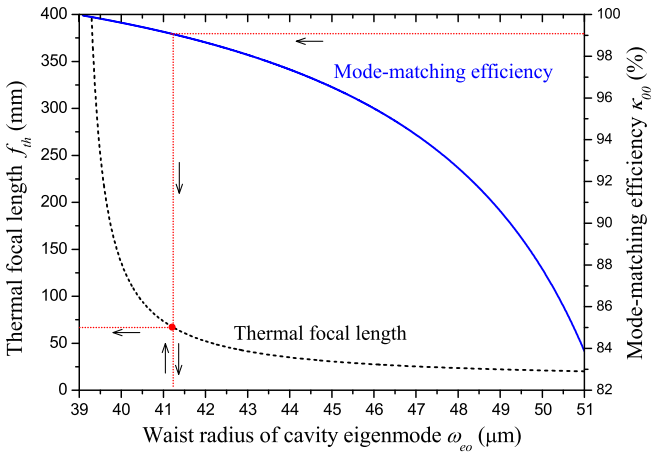

Fig. 1. Theoretical relationship between eigenmode waist radius, mode-matching efficiency and thermal focal length.

The solid curve in Fig. 1 shows the dependence of the mode-matching efficiency on the eigenmode waist radius (ω_{e0}) of the external optical cavity. A clear correspondence between the thermal focal length (left vertical axis of Fig. 1) and mode-matching efficiency (right vertical axis of Fig. 1) is constructed through the eigenmode waist radius (ω_{e0}) of the external optical cavity (horizontal axis of Fig. 1) as an intermediate variable.

Before injecting the harmonic wave beam into the PPKTP crystal (the thermal focal length equals infinity), the initial mode-matching efficiency should be optimized to reach a mode-matching efficiency of 100% to eliminate the influence of the non-monotonic mode-matching efficiency with the harmonic wave power. However, in reality, the optimization of the initial mode-matching efficiency, which is limited by the focal length of the lens available in a laboratory, the available space in the optical setup and lens errors, can be close to 100% but not be achieved. The initial mode-matching efficiency can be summed up in two cases. Case one: $\omega_{s0} < \omega_{e0}$; with increasing harmonic wave power, the thermal focal length gradually shortens, and the eigenmode waist radius ω_{e0} of the external optical cavity increases monotonically, which decreases the mode-matching efficiency monotonically. There is a one-to-one correspondence between mode-matching efficiency and thermal focal length. Case two: $\omega_{s0} > \omega_{e0}$; with increasing harmonic wave power, the thermal focal length decreases, and ω_{e0} increases monotonically, which will smoothly increase mode-matching efficiency to 100%, and then it decreases. In this case, there may be two thermal focal lengths for one mode-matching efficiency: one corresponding to the upward

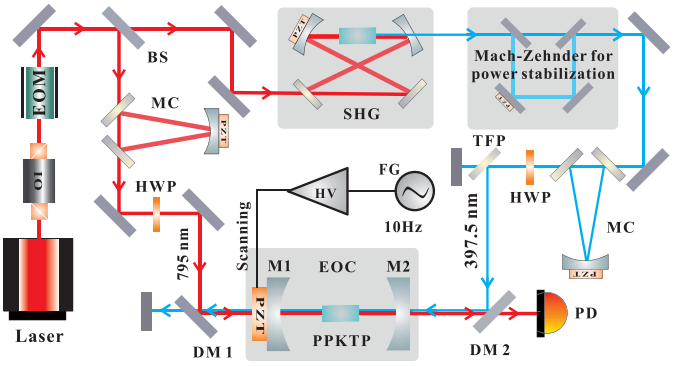

Fig. 2. Simplified sketch of the experimental setup for thermal lens measurement. EOC: external optical cavity; EOM: electro-optical modulator; OI: optical isolator; SHG: second harmonic generator; HWP: half-wave plate; FG: function generator; HV: high-voltage amplifier; PD: photodiode detector; DM: dichroic mirror; M1-2: concave mirrors 1-2 for the resonator; PZT: piezoelectric transducer; MC: mode cleaner; BS: beam splitter; TFP: thin-film polarizer.

stage of mode-matching efficiency, and the other corresponding to the downward stage.

For case two, the mode-matching efficiency cannot exclusively determine the thermal focal length; we should avoid this case in an actual measurement. For case one, the thermal focal length has a one-to-one correspondence with the mode-matching efficiency, which can be uniquely determined. During the process of an actual measurement, the two cases can be distinguished by observing the monotonicity between the mode-matching efficiency and harmonic wave power. By presetting the thermal focal length measurement to case one, the one-to-one correspondence of $P_{2\omega} \rightarrow f_{th} \rightarrow \omega_{e0} \rightarrow \kappa_{00}$ is confirmed, and the thermal focal length is obtained. Based on the above theoretical analysis, it implies that the initial mode-matching efficiency has no influence on the thermal focal length measurement. However, in practical experiments, there are several reasons to influence the mode-matching efficiency value. If the initial mode-matching efficiency is low, we cannot exclude the influence of the input beam misalignment and waist position mismatching on the mode-matching efficiency. Therefore, the initial mode-matching efficiency should be greater than 99% to minimize the influence described above.

III. Experimental Setup

Fig. 2 illustrates the experimental setup for measuring the thermal focal length of a PPKTP crystal through an external optical cavity. The cavity is composed of two concave mirrors (M1 and M2 with a curvature radius of 30 mm). A PPKTP crystal with dimensions of $1\times2\times10$ mm as a measured material is placed inside the cavity, and its two end facets are coated with a double antireflection (AR) coating at 795 nm and 397.5 nm. The cavity's length is 57.5 mm, corresponding to a waist radius of 38.9 μm at 795 nm or 27.6 μm at 397.5 nm, and the PPKTP crystal is placed at the waist position of the cavity. The concave end face of M1 is coated with a partly transmission coating $T_{795} = 3.6\%$ at 795 nm and a high transmission (HT) coating at 397.5 nm. The concave end face of M2 is coated with a high reflectivity (HR) coating at 795 nm and HT at 397.5 nm. The plane faces of both M1 and M2 are AR coated at both wavelengths. The harmonic wave does not resonate inside the cavity.

The laser source is a home-made Ti:sapphire laser with a wavelength of 795 nm [40], which is pumped by a home-made high-power single-frequency 532 nm laser with a maximum output power of 20 W [25], [41]. The output power at 795 nm is 1.27 W, and a small portion of the laser is used as the seed beam (fundamental wave) for the mode-matching efficiency measurement. The retained large power is sent into the frequency doubler to produce a continuous wave single-frequency laser at 397.5 nm (harmonic wave) via the SHG process [3]. In practical thermal focal length measurements, any HW power change, beam pointing fluctuations or poor beam quality will deviate the mode-matching efficiency from the actual value at certain power [37] due to a variation in heat generation or a misalignment of the optical cavity, which potentially distorts the measured result of the thermal lens. To avoid the additional system error above, the harmonic wave is guided into a Mach-Zehnder-type interferometer to improve its power stability. Subsequently, a mode cleaner (MC) is inserted before the cavity to ensure that the HW field injected into it is a pure TEM_{00} mode and has a good pointing stability. This scheme reduces the measurement error arising from power and pointing fluctuations of the harmonic wave [42]. Similarly, another MC is also adopted to improve the spatial mode and pointing stability of the fundamental wave to exclude the potential deviation of the mode-matching efficiency originating from beam quality and pointing noise. A combination of a half-wave plate (HWP) and a thin-film polarizer (TFP) forms an attenuation unit and allows us to adjust the harmonic wave power for heating the PPKTP crystal. The setup here is a part of the 795 nm squeezer, which aims to obtain a high degree of squeezed states for the rubidium D1 line [34].

A triangular wave signal from a function generator (FG) is employed to scan the length of the external optical cavity, with which transmission peaks of the cavity will be obtained by applying high voltage to the piezoelectric transducer (PZT). A photodetector (PD) is used to observe the transmission peaks among a free spectral range (FSR) of the cavity, whose output is connected to an oscilloscope to record the transmission curve for calculating the mode-matching efficiency. Dichroic mirror 1 (DM1) is coated with HR at 795 nm and HT at 397.5 nm, and DM2 is coated with HT at 795 nm and HR at 397.5 nm to separate the fundamental wave from the harmonic wave.

IV. Experimental Results

We conduct the thermal focal length measurement as follows. First, a 795 nm laser of approximately 1 mW in pure fundamental mode is aligned and mode matched to the cavity from M1. The low power level ensures little heat contribution to the thermal lens of the material, in which only SHG is considered for the thermal lens measurement. The mode-matching efficiency between the 795 nm laser mode and the TEM_{00} eigenmode of the cavity can be obtained by counting the intensity ratio of the main transmission peak to all the transmission peaks among a FSR of the cavity. Before

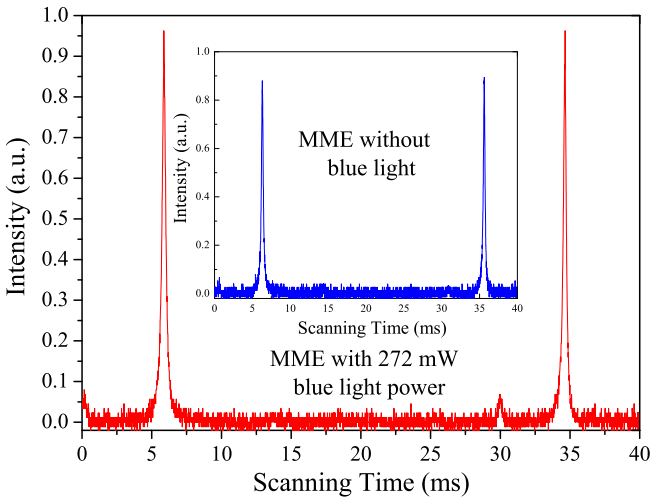

Fig. 3. Normalized transmission peaks of cavity scanning for seed wave without harmonic wave and with harmonic wave power of 272 mW.

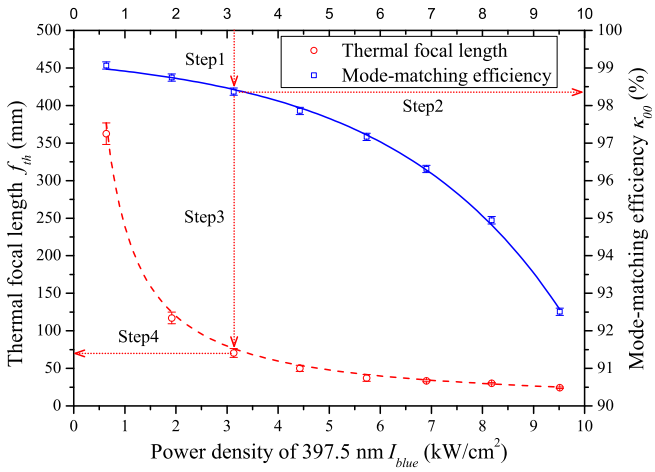

Fig. 4. Measurement results of thermal focal length and mode-matching efficiency for different harmonic wave powers. Step 1: selecting a harmonic wave power; Step 2: measuring the corresponding mode-matching efficiency; Step 3: calculating the thermal focal length; Step 4: constructing the relationship between mode-matching efficiency and thermal focal length.

injecting the harmonic wave beam, the initial mode-matching efficiency is optimized to 99.2%, which is shown in the inset of Fig. 3. Subsequently, the 397.5 nm beam is adjusted to overlap with the 795 nm beam and is focused on the center of the PPKTP crystal with a waist radius of approximately 27.6 μm. We increase the laser power of 397.5 nm slowly, and then the variation trend of the mode-matching efficiency is observed. When we gradually increase the harmonic wave power from 0 to 272 mW, the mode-matching efficiency monotonically decreases from 99.2% to 92.5%, corresponding to case one in section 2, which shows a one-to-one correspondence between the mode-matching efficiency and thermal focal length. Fig. 3 shows the transmission curve of the cavity scanning among a FSR at the harmonic wave power of 272 mW. To quantify the relation of the thermal focal length and mode-matching efficiency experimentally, we adjust the harmonic wave power from 18 mW ($I_{2\omega} = 0.64$ kW/cm^2) to 272 mW ($I_{2\omega} = 9.5$ kW/cm^2) in power intervals of approximately 36 mW, and the mode-matching efficiency is calculated based on the transmission curve at each power. The squares in Fig. 4 present the measurement results of the mode-matching efficiency for individual power levels, and this figure clearly shows that the mode-matching efficiency becomes worse and is accompanied by an increase in the harmonic wave power density.

By means of the intermediate quantity of the cavity's eigenmode, f_{th} can be inferred from the measured values of κ_{00}, which follows the process of $f_{th} \rightarrow \omega_{e0} \rightarrow \kappa_{00}$. According to the parameters described above, the dependency of f_{th} (unit: mm) and κ_{00} can be expressed as follows:

$$f_{th} = 17.21108 + \frac{0.46765}{0.992 - \kappa_{00}} \tag{9}$$

Based on this expression and the measured results of the mode-matching efficiency, the thermal focal length can be obtained at each power density, which are shown as circular symbols in Fig. 4. When the injected harmonic wave power density increases from 0.64 kW/cm^2 to 9.5 kW/cm^2, the observed mode-matching efficiency gradually decreases from approximately 99.1% to 92.5% (square symbols in Fig. 4), and the corresponding thermal focal length transforms from 362.6 mm to 24.2 mm. For this case, the thermal focal length varies the eigenmode size, and furthermore, it deteriorates the mode-matching efficiency between the fundamental wave beam and cavity's eigenmode, which is quite harmful to the nonlinear interaction in the PPKTP crystal. Our method can obtain not only the thermal focal length of the material but also the mode-matching efficiency variation of the optical cavity, which is helpful for comprehensively evaluating the influence of the thermal lens effect on the frequency up-conversion and down-conversion processes and proposing some effective actions for overcoming it. The overall statistical and systematic errors are determined through an inaccuracy measurement of the mode-matching efficiency, optical power, and initial waist radius (or position) of the resonant beam. However, due to the initial mode-matching efficiency being close to 100%, the influence of the waist position discrepancy on the initial mode-matching efficiency can be ignored, and only the waist radius discrepancy is considered. To estimate the total experimental errors for the thermal focal length measurement, more than 10 mode-matching efficiencies at each harmonic wave power level were measured, and the average values are fitted with a solid line in Fig. 4. The theoretical thermal focal length obtained by Eq. (1) is shown with a dashed line in Fig. 4, in which the experiment results slightly deviate from the theoretical values. The error bars are determined by the standard deviation of the experimental data. The measured results agree well with the theoretical values within the overall errors. The theoretical and experimental results also show that the mode-matching efficiency intensely changes at higher harmonic wave power density, which makes the thermal focal length measurement more sensitive to the power density at higher harmonic wave power. Therefore, our mensuration of the thermal focal length is more accurate for high power density measurements.

V. Conclusion

The experimental setup enables the thermal focal length measurement of a nonlinear crystal during the processes of SHG and OPO, which can represent the thermal focal length under working conditions. The thermal focal length is obtained by observing the deviation in the mode-matching efficiency from the initial value in an external optical cavity, which results from the eigenmode size variation originating from the thermal lens of a PPKTP crystal. For an external optical cavity, the thermal focal length affects its eigenmode size, whereas it deteriorates the mode-matching efficiency between the fundamental wave beam and the cavity eigenmode, which is quite harmful to the nonlinear interaction. Based on the theoretical and experimental results, the deterioration of the mode-matching efficiency of the cavity becomes more severe at higher harmonic wave power density, which leads to a more sensitive measurement for thermal focal length at higher harmonic wave power. Therefore, the measurement of the thermal focal length will become more accurate with high laser intensity exposure. Our method can obtain not only the thermal focal length of the material but also the mode-matching efficiency variation of the optical cavity, which is helpful for comprehensively evaluating the influence of the thermal lens effect on the up-conversion and down-conversion processes. Consequently, the eigenmode size variation and mode-matching efficiency deviation coming from the thermal lens can be thoroughly considered and characterized to optimize the cavity design for both SHG and OPO.

References

[1] A. Zukauskas, V. Pasiskevicius, and C. Canalias, "Second-harmonic generation in periodically poled bulk Rb-doped $KTiOPO_4$ below 400 nm at high peak-intensities," *Opt. Exp.*, vol. 21, no. 2, pp. 1395–1403, Jan. 2013.

[2] X. Wen *et al.*, "Cavity-enhanced frequency doubling from 795 nm to 397.5 nm ultra-violet coherent radiation with PPKTP crystals in the low pump power regime," *Opt. Exp.*, vol. 22, no. 26, pp. 32293–32300, Dec. 2014.

[3] W. Yang, Y. Wang, Y. Zheng, and H. Lu, "Comparative study of the frequency-doubling performance on ring and linear cavity at short wavelength region," *Opt. Exp.*, vol. 23, no. 15, pp. 19624–19633, Jul. 2015.

[4] S. Ast *et al.*, "High-efficiency frequency doubling of continuous-wave laser light," *Opt. Lett.*, vol. 36, no. 17, pp. 3467–3469, Sep. 2011.

[5] Y. Takeno, M. Yukawa, H. Yonezawa, and A. Furusawa, "Observation of -9 dB quadrature squeezing with improvement of phase stability in homodyne measurement," *Opt. Exp.*, vol. 15, no. 7, pp. 4321–4327, Apr. 2007.

[6] S. Ast, M. Mehmet, and R. Schnabel, "High-bandwidth squeezed light at 1550 nm from a compact monolithic PPKTP cavity," *Opt. Exp.*, vol. 21, no. 11, pp. 13572–13579, Jun. 2013.

[7] Y. H. Zheng, Z. Q. Wu, M. R. Huo, and H. J. Zhou, "Generation of a continuous-wave squeezed vacuum state at 1.3 μm by employing a home-made all-solid-state laser as pump source," *Chin. Phys. B*, vol. 22, no. 9, p. 094206, Mar. 2013.

[8] H. Mabuchi, E. S. Polzik, and H. J. Kimble, "Blue-light-induced infrared absorption in $KNbO_3$," *J. Opt. Soc. Amer. B*, vol. 11, no. 10, pp. 2023–2029, Oct. 1994.

[9] L. Shiv, J. L. Sorensen, E. S. Polzik, and G. Mizell, "Inhibited light-induced absorption in $KNbO_3$," *Opt. Lett.*, vol. 20, no. 22, pp. 2270–2272, Nov. 1995.

[10] V. A. Maslov, V. A. Mikhailov, O. P. Shaunin, and I. A. Shcherbakov, "Nonlinear absorption in KTP crystals," *Quantum Electron.*, vol. 27, no. 4, pp. 356–359, Nov. 1997.

[11] J. Hirohashi, V. Pasiskevicius, S. Wang, and F. Laurell, "Picosecond blue light-induced infrared absorption in single-domain and periodically poled ferroelectrics," *J. Appl. Phys.*, vol. 101, no. 3, p. 033105, Feb. 2007.

[12] S. G. Sabouri, C. Suddapalli, A. Khorsandi, and M. Ebrahim-Zadeh, "Thermal effects in high-power continuous-wave single-pass second harmonic generation," *IEEE J. Sel. Topics Quantum Electron.*, vol. 20, no. 5, Jan. 2014, Art. no. 7500210.

[13] U. O. Farrukh, A. M. Buoncristiani, and C. E. Byvik, "An analysis of the temperature distribution in finite solid-state laser rods," *IEEE J. Quantum Electron.*, vol. 24, no. 11, pp. 2253–2263, Nov. 1988.

[14] Y. F. Chen, T. M. Huang, C. F. Kao, C. L. Wang, and S. C. Wang, "Optimization in scaling fiber-coupled laser-diode end-pumped lasers to higher power: Influence of thermal effect," *IEEE J. Quantum Electron.*, vol. 33, no. 8, pp. 1424–1429, Aug. 1997.

[15] A. K. Cousins, "Temperature and thermal stress scaling in finite-length end-pumped laser rods," *IEEE J. Quantum Electron.*, vol. 28, no. 4, pp. 1057–1069, Apr. 1992.

[16] M. E. Innocenzi, H. T. Yura, C. L. Fincher, and R. A. Fields, "Thermal modeling of continuous-wave end-pumped solid-state lasers," *Appl. Phys. Lett.*, vol. 56, no. 19, pp. 1831–1833, May 1990.

[17] M. Sabaeian, F. S. Jalil-Abadi, M. M. Rezaee, and A. Motazedian, "Heat coupled Gaussian continuous-wave double-pass type-II second harmonic generation: Inclusion of thermal induced phase mismatching and thermal lensing," *Opt. Exp.*, vol. 22, no. 21, pp. 25615–25628, Oct. 2014.

[18] L. Mousavi, M. Sabaeian, and H. Nadgaran, "Thermal-induced birefringence in solid-core photonic crystal fiber lasers," *Opt. Commun.*, vol. 300, pp. 69–76, Apr. 2013.

[19] M. Sabaeian, F. S. Jalil-Abadi, M. M. Rezaee, A. Motazedian, and M. Shahzadeh, "Temperature increase effects on a double-pass cavity type II second-harmonic generation: A model for depleted Gaussian continuous waves," *Appl. Opt.*, vol. 54, no. 4, pp. 869–875, Feb. 2015.

[20] M. M. Rezaee, M. Sabaeian, A. Motazedian, F. S. Jalil-Abadi, H. Askari, and I. Khazrk, "Thermally induced phase mismatching in a repetitively Gaussian pulsed pumping KTP crystal : A spatiotemporal treatment," *Appl. Opt.*, vol. 54, no. 15, pp. 4781–4788, May 2015.

[21] G. Hansson, H. Karlsson, S. H. Wang, and F. Laurell, "Transmission measurements in KTP and isomorphic compounds," *Appl. Opt.*, vol. 39, no. 27, pp. 5058–5069, Sep. 2000.

[22] Z. M. Liao *et al.*, "Thermally induced dephasing in periodically poled KTP frequency-doubling crystals," *J. Opt. Soc. Amer. B*, vol. 21, no. 12, pp. 2191–2196, Dec. 2004.

[23] M. Sabaeian, L. Mousave, and H. Nadgaran, "Investigation of thermally-induced phase mismatching in continuous-wave second harmonic generation: A theoretical model," *Opt. Exp.*, vol. 18, no. 18, pp. 18732–18743, Aug. 2010.

[24] S. G. Sabouri, C. K. Suddapalli, A. Khorsandi, and M. Ebrahim-Zadeh, "Focusing optimization for high-power continuous-wave second-harmonic generation in the presence of thermal effects," *IEEE J. Sel. Topics Quantum Electron.*, vol. 21, no. 1, Jan. 2015, Art. no. 1602808.

[25] Y. J. Wang, Y. H. Zheng, Z. Shi, and K. C. Peng, "High-power single-frequency Nd:YVO_4 green laser by self-compensation of astigmatisms," *Laser Phys. Lett.*, vol. 9, no. 7, pp. 506–510, Jun. 2012.

[26] S. Fan, X. Zhang, Q. Wang, S. Li, S. Ding, and F. Su, "More precise determination of thermal lens focal length for end-pumped solid-state lasers," *Opt. Commun.*, vol. 266, no. 2, pp. 620–626, Oct. 2006.

[27] W. Koechner, "Thermal lensing in a Nd:YAG laser rod," *Appl. Opt.*, vol. 9, no. 11, pp. 2548–2553, Nov. 1970.

[28] P. J. Hardman, W. A. Clarkson, G. J. Friel, M. Pollnau, and D. C. Hanna, "Energy-transfer upconversion and thermal lensing in high-power end-pumped Nd:YLF laser crystals," *IEEE J. Quantum Electron.*, vol. 35, no. 4, pp. 647–655, Apr. 1999.

[29] B. Neuenschwander, R. Weber, and H. P. Weber, "Determination of the thermal lens in solid-state lasers with stable cavities," *IEEE J. Quantum Electron.*, vol. 31, no. 6, pp. 1082–1087, Jun. 1995.

[30] F. Song *et al.*, "Determination of thermal focal length and pumping radius in gain medium in laser-diode-pumped Nd:YVO_4 lasers," *Appl. Phys. Lett.*, vol. 81, no. 12, pp. 2145–2147, Sep. 2002.

[31] J. Zou, S. Zhao, K. Yang, and G. Li, "A simple method to determine the thermal focal length of solid-state lasers with rate equation," *Opt. Laser Techol.*, vol. 39, no. 4, pp. 778–781, Jan. 2007.

[32] J. L. Blows, J. M. Dawes, and T. Omatsu, "Thermal lensing measurements in line-focus end-pumped neodymium yttrium aluminium garnet using holographic lateral shearing interferometry," *J. Appl. Phys.*, vol. 83, no. 6, pp. 2901–2906, Dec. 1998.

[33] C. Bogan, P. Kwee, S. Hild, S. H. Huttner, and B. Willke, "Novel technique for thermal lens measurement in commonly used optical components," *Opt. Exp.*, vol. 23, no. 12, pp. 15380–15389, Jun. 2015.
[34] Z. Xu *et al.*, "Long lifetime and high-fidelity quantum memory of photonic polarization qubit by lifting zeeman degeneracy," *Phys. Rev. Lett.*, vol. 111, no. 24, p. 240503, Dec. 2013.
[35] J. Steinlechner *et al.*, "Absorption measurements of periodically poled potassium titanyl phosphate (PPKTP) at 775 nm and 1550 nm," *Sensors*, vol. 13, no. 1, pp. 565–573, Jan. 2013.
[36] CASTECH Inc., *KTP-KTP-Crystal Products*, accessed on Sep. 9, 2016. [Online]. Available: http://www.castech.com/products_detail/&productId=99.html
[37] D. Z. Anderson, "Alignment of resonant optical cavities," *Appl. Opt.*, vol. 23, no. 17, pp. 2944–2949, 1984.
[38] N. Uehara, E. K. Gustafson, M. M. Fejer, and R. L. Byer, "Modeling of efficient mode matching and thermal-lensing effect on a laser-beam coupling into a mode-cleaner cavity," *Proc. SPIE*, vol. 2989, pp. 57–68, Feb. 1997.
[39] T. Klaassen, J. D. Jong, M. V. Exter, and J. P. Woerdman, "Transverse mode coupling in an optical resonator," *Opt. Lett.*, vol. 30, no. 15, pp. 1959–1961, 2005.
[40] H. Lu, X. Sun, M. Wang, J. Su, and K. Peng, "Single frequency Ti:Sapphire laser with continuous frequency-tuning and low intensity noise by means of the additional intracavity nonlinear loss," *Opt. Exp.*, vol. 22, no. 20, pp. 24551–24558, Oct. 2014.
[41] Y. Wang, W. Yang, H. Zhou, M. Huo, and Y. Zheng, "Temperature dependence of the fractional thermal load of Nd:YVO_4 at 1064 nm lasing and its influence on laser performance," *Opt. Exp.*, vol. 21, no. 15, pp. 18068–18078, Jul. 2013.
[42] A. Khalaidovski *et al.*, "Long-term stable squeezed vacuum state of light for gravitational wave detectors," *Class. Quantum Gravity*, vol. 29, no. 7, p. 075001, Mar. 2012.

Yajun Wang received the Ph.D. degree in physics from Shanxi University, Shanxi, China, in 2014.

He is currently a Researcher with the Institute of Opto-Electronics, Shanxi University. His research interests include high-power single-frequency lasers, quantum optics devices, and nonlinear optics.

Zhixiu Li received the B.S. degree in physics from Yuncheng University, Shanxi, China, in 2013. She is currently pursuing the Ph.D. degree with the Institute of Opto-Electronics, Shanxi University, China.

Her main research interests include quantum optics devices and nonlinear optics.

Yaohui Zheng was born in 1979. He received the M.S. degree in optical engineering and the Ph.D. degree in laser technology from Shanxi University, China, in 2004 and 2009, respectively.

He is currently a Researcher with the Institute of Opto-Electronics, Shanxi University. His current research interests include high-power single frequency lasers, quantum optics devices, and nonlinear optics.

Jing Su was born in 1979. She received the Ph.D. degree in laser technology from Nankai University, China, in 2007.

She is currently a Researcher with the Institute of Opto-Electronics, Shanxi University, China. Her current research interests include high-power single frequency lasers, quantum optics devices, and nonlinear optics.